Journal of Peptide Science
*J. Peptide Sci.* **9**: 386–392 (2003)
Published online in Wiley InterScience (www.interscience.wiley.com). DOI: 10.1002/psc.465

JOURNAL OF PEPTIDE SCIENCE

# Nascent Helix in the Multiphosphorylated Peptide $\alpha_{S2}$-Casein(2–20)

**N. LAILA HUQ, KEITH J. CROSS and ERIC C. REYNOLDS***

School of Dental Science, The University of Melbourne, 711 Elizabeth Street, Melbourne, 3000, Victoria, Australia

*Received 12 November 2002*
*Accepted 19 February 2003*

Abstract: Sequence-specific nuclear magnetic resonance (NMR) assignments have been determined for the peptide $\alpha_{S2}$-CN(2–20) containing the multiphosphorylated motif-$^{8}$Ser(*P*)-Ser(*P*)-Ser(*P*)-Glu-Glu$^{12}$- in the presence of molar excess $Ca^{2+}$. The secondary structure of the peptide was characterized by sequential (i,i + 1), medium-range (i,i + 2/3/4) nOes and H$\alpha$ chemical shifts. Molecular modelling of the peptide based on these constraints suggests a nascent helix for residues Ser(*P*)$^{9}$ to Glu$^{12}$. The spectral data for $\alpha_{S2}$-CN(2–20) were compared with those of other casein phosphopeptides $\beta$-CN(1–25) and $\alpha_{S1}$-CN(59–79) that also contain the multiphosphorylated motif. This comparison revealed a similar pattern of secondary amide chemical shifts in the multiphosphorylated motif. However, the patterns of medium-range nOe connectivities in the three peptides suggests they have distinctly different conformations in the presence of $Ca^{2+}$ despite having a high degree of sequential similarity. 

Keywords: casein phosphopeptide; $\alpha_{S2}$-CN(2–20); $^{1}$H NMR; structure

## INTRODUCTION

Multi-site, hierarchical protein phosphorylation is a prevalent form of protein modification. It has been suggested that this type of modification allows for regulation of protein activity by expanding the structural repertoire [1] The sequence -S-S-S-E-E- occurs in over 200 protein sequences [2]. The proteins containing this sequence include not only the caseins, but also a variety of growth factors, kinases, immunoglobins, and nuclear regulatory proteins. This sequence has the potential to be phosphorylated by the ordered action of a mammary gland-like kinase that recognizes the motif -S-X-E/S(*P*)- or to be partially phosphorylated by casein kinase II that recognizes the sequence -S-X-X-E/S(*P*)- [1]. Furthermore, some of the proteins have acidic residues flanking both sides of the serine cluster, for example -E-E-S-S-S-E-E-, such that the seryl residues may be completely phosphorylated by the combined action of casein kinases I and II, where casein kinase I recognizes the motif-E/S(*P*)-X-X-S- [1]. Notwithstanding the frequency with which the -S-S-S-E-E- motif occurs in proteins and the potential for phosphorylation very little is known about the conformational preferences of multiphosphorylated sequences.

Multiphosphorylated proteins play an important role in the processes of biomineralization. In the development of teeth they act as nucleators of

Abbreviations: ACP, amorphous calcium phosphate; CN, casein; Σ, O-phosphorylated serine; 2D, two-dimensional; DQF-COSY, 2D correlated spectroscopy using double-quantum filter; NMR, nuclear magnetic resonance; nOe, nuclear Overhauser effect; NOESY, 2D nuclear Overhauser and exchange spectroscopy.

*Correspondence to: Professor Eric C. Reynolds, School of Dental Science, The University of Melbourne, 711 Elizabeth Street, Melbourne, Victoria, 3000, Australia;
e-mail: e.reynolds@unimelb.edu.au
Contract/grant sponsor: NH&MRC; Contract/grant number: 209042.
Contract/grant sponsor: Dairy Research and Development Corporation of Australia.

hydroxyapatite and control the growth of the crystals resulting in a unique crystal morphology. In body fluids such as saliva and milk, multiphosphorylated proteins stabilize amorphous calcium phosphate (ACP) phases in metastable solution. In milk, ACP is stabilized in micelles in combination with the caseins (CN). The caseins act as sources of bioactive peptides and nutrients for the neonate upon digestion. The calcium-sensitive caseins that are responsible for binding to ACP are characterized by clusters of acidic residues, including the fully phosphorylated sequence motif SSSEE. The phosphorylated motif is found in the calcium-sensitive bovine caseins: $\alpha_{S1}$-, $\alpha_{S2}$- and $\beta$-casein and in the tryptic peptides $\alpha_{S1}$-CN(59–79), $\beta$-CN(1–25) and $\alpha_{S2}$-CN(2–20) released during digestion (Figure 1). The tryptic peptides sequester their own weight in ACP to form colloidal complexes [3] and are found in the soluble part of the intestinal chyme after digestion [4,5] and even in the faeces [6] of experimental animals due to proteolytic resistance of the peptides. The ACP binding properties of the tryptic casein phosphopeptides coupled with their ability to form soluble complexes supports a biological role as calcium carriers [7]. These peptides also exhibit anticariogenic activity through their ability to stabilize and localize ACP at the tooth surface thereby inhibiting enamel demineralization and promoting enamel remineralization [8–10].

We have previously reported the structural features of $\alpha_{S1}$-CN(59–79) and $\beta$-CN(1–25) derived from proton NMR spectroscopic studies [11,12]. These studies showed that although these peptides exhibit sequence similarities, in particular the -Σ-Σ-Σ-E-E- motif, they displayed different conformational preferences in the presence of calcium ions. The aim of the present study was to determine the conformational preferences of another tryptic casein multiphosphorylated peptide, $\alpha_{S2}$-CN(2–20) containing -Σ-Σ-Σ-E-E- motif using $^1$H NMR spectroscopy and to compare these structural features with those of $\alpha_{S1}$-CN(57–59) and $\beta$-CN(1– 25).

| | |
|---|---|
| $^{59}$QMEAEΣIΣΣΣEEIVPNΣVEQK$^{79}$ | $\alpha_{S1}$-CN(59-79) |
| $^{1}$RELEELNVPGEIVEΣLΣΣΣEESITR$^{25}$ | β-CN(1-25) |
| $^{2}$NTMEHVΣΣΣEESIIΣQETY$^{20}$ | $\alpha_{S2}$-CN(2-20) |

Figure 1 Primary structures of the tryptic casein multiphosphorylated peptides $\alpha_{S1}$-CN(59–79), $\beta$-CN(1–25) and $\alpha_{s2}$-CN(2–20) using the one letter code with the symbol Σ representing Ser(*P*). The multiphosphorylated sequence ΣΣΣEE common to these peptides is underlined.

## MATERIALS AND METHODS

### Peptide Purification

The casein phosphopeptide $\alpha_{S2}$-CN(2–20) was selectively precipitated from a tryptic digest of casein using $Ca^{2+}$ and ethanol and further purified by anion exchange FPLC and reversed phase HPLC [13]. The purity of the peptide was checked by amino acid sequencing [13], capillary electrophoresis [14] and mass spectrometry [15] as previously described. A 10.7 mM peptide solution was prepared at pH 6.36 in 90% $H_2O$/10% $D_2O$.

### $^1$H NMR Spectroscopy

All spectra were recorded with spectral widths of 6000.6 Hz in $F_1$ and $F_2$ with 1024 complex data points. Phase-sensitive spectra were collected using the States-TPPI method [16]. The WET [17] pulse sequence was used for solvent suppression in the NOESY [18,19] and TOCSY [20,21] spectra. Presaturation of the solvent peak was used when acquiring the DQF-COSY [22,23] spectra. Mixing times of 250 ms and 300 ms were used in acquiring the NOESY spectra and a mixing time of 80 ms was used for the TOCSY spectrum. A total of 100 $t_1$ increments of 16 transients were collected for the TOCSY spectrum. The 250 ms NOESY had 128 $t_1$ increments of 128 transients while the 300 ms NOESY had 200 $t_1$ increments of 64 transients. The DQF-COSY spectra had 200 $t_1$ increments of 4 transients.

NOESY and TOCSY spectra were zero-filled to 2k complex points in $t_2$ prior to Fourier transformation. Linear prediction was used to extrapolate the $t_1$ data to 2k data points. A Hamming window function [24] was applied to both the $t_1$ and $t_2$ data. The DQ-COSY spectra were zero-filled to 2k complex points in $t_2$ and to 1024 complex points in $t_1$. A sine-bell window function was applied to both $t_2$ and $t_1$ data. All data processing was performed using Varian's VnmrS program on an SGI Indigo$^2$ workstation with 256 MBytes of RAM.

### Molecular Modelling

All calculations were performed with the molecular modelling software package SYBYL 6.8 (Tripos Associates, St Louis, MO, USA) on a Silicon Graphics Octane workstation. The Kollman all atom forcefield was utilized without the electrostatic term with no cutoff for nonbonded interactions. The *in*

*silico* $\alpha_{S2}$-CN(2–20) peptide was constructed using the biopolymer function. Torsion constraints were added to maintain *trans* peptide bonds and the chirality of chiral centres. Simulated annealing was carried out as implemented in SYBYL (50 cycles consisting of heating to 2000 K, equilibration at 2000 K for 50 ps and exponential cooling from 2000 K to 50 K for 5000 fs). Procheck was used to check angles. The 50 structures obtained were minimized using the Kollman all atom forcefield and no cut-off for nonbonded interactions. The local geometry of each of the ten lowest energy structures was checked. For each structure, conformational analysis was performed using Ramachandran plots, and the nOe violations were examined. Finally RMSD calculations of the 10 lowest energy structures were performed taking into consideration only the heavy backbone atoms of selected residues.

## RESULTS AND DISCUSSION

### Assignment of Spin Systems

The amino acid spin systems of $\alpha_{S2}$-CN(2–20) were identified by examining the DQF-COSY, TOCSY and NOESY recorded in $H_2O$ at pH 6.36 at a temperature of −5 °C. The single histidine, valine, asparagine and serine, two isoleucines, and three phosphoserines were recognized by their chemical shifts and the connectivity patterns in the DQF-COSY spectrum [25]. The $\beta H_2$ to NH nOes of the four *O*-phosphoserines were observed in the fingerprint region of the TOCSY and NOESY permitting their sequence specific assignments. The $\alpha$H-NH intra-residue crosspeak between $N^2$ and $T^3$ was not observed. The nOe crosspeaks connecting the side-chain amide resonances of $N^2$ and $Q^{17}$ were observed and sequentially assigned. Figures 2 and 3 show the fingerprint and amide regions respectively of the NOESY spectrum with the sequential and non-sequential nOes highlighted.

### Effect of Calcium on Spectra of $\alpha_{S2}$-CN(2–20)

The presence of calcium ions induced changes in the chemical shifts of resonances in the fingerprint region of $\alpha_{S2}$-CN(2–20) at pH 6.36 (Figure 4). Table 1 lists the chemical shifts of $\alpha_{s2}$-CN(2–20) in the presence of calcium ions. The amide protons of residues $H^6$, $\Sigma^9$, were shifted toward lower frequencies, whereas the amide protons of $E^{12}$, $I^{15}$, $\Sigma^{16}$ were shifted toward higher frequencies. The H$\alpha$ protons of $M^4$, $V^7$, $\Sigma^8$, $\Sigma^{10}$, $E^{12}$, $\Sigma^{16}$ and $E^{18}$ show significant shifts toward lower frequencies, whereas the H$\alpha$ protons of $\Sigma^9$ and $I^{14}$ show significant shifts toward higher frequencies.

The secondary H$\alpha$ and NH proton chemical shifts of the phosphoseryl residues were calculated using the 'random coil' chemical shifts

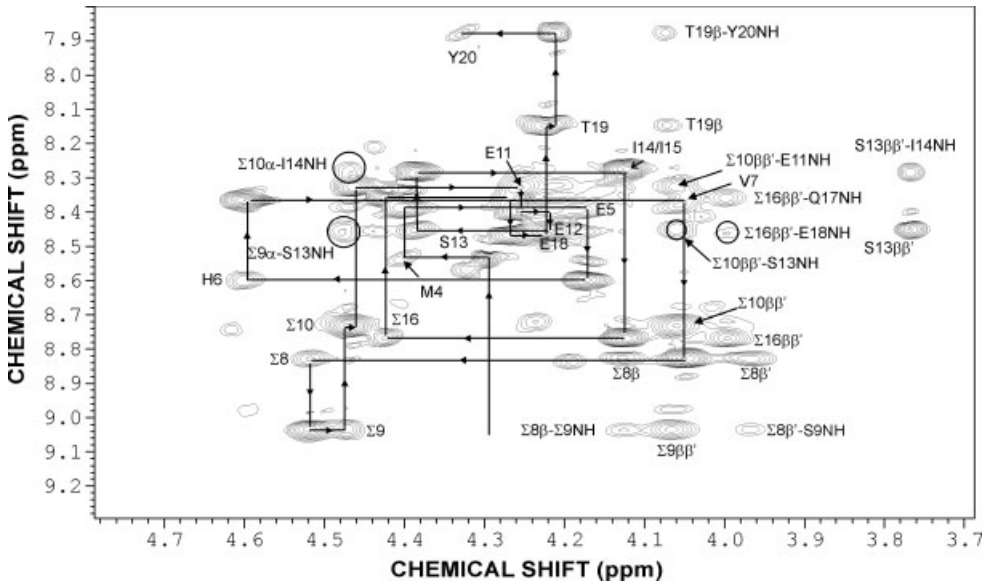


Figure 2 Fingerprint region of a NOESY spectrum of $\alpha_{S2}$-CN(2–20) recorded in 80% $H_2O$/20% $D_2O$. Non-sequential nOes are circled. The spectrum was recorded using 10 mM peptide, pH 6.36 at −5 °C with 4 mol $Ca^{2+}$/mol peptide. The mixing time was 300 ms.

 

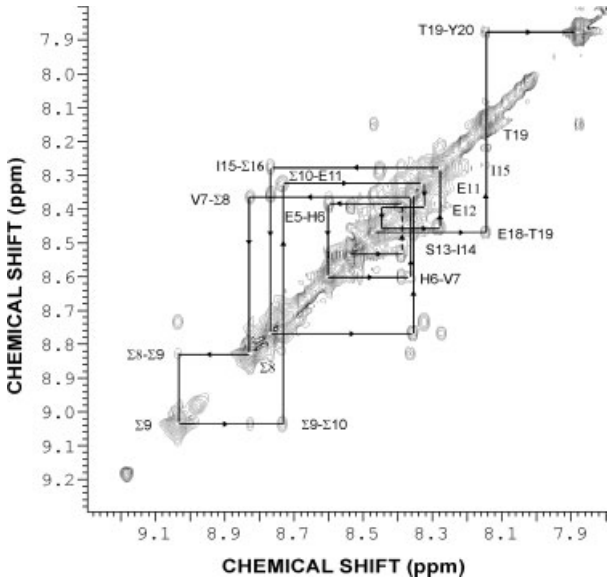


Figure 3 The amide region of the NOESY spectrum showing sequential connectivity. Sample conditions are summarized in the caption to Figure 2. I14/I15 can not be distinguished by their amide shifts.

reported by Bienkiewicz and Lumb [26]. The secondary Hα and NH proton chemical shifts of the other residues were calculated using the 'random coil' chemical shifts reported by Merutka *et al.* [27] with the sequence-dependent corrections recently reported by Schwarzinger *et al.* [28].

Figure 5(a,b) shows the secondary Hα and amide chemical shifts. The amide protons of $T^3$ were shifted towards lower frequencies, whereas the Hα and amide protons of the $M^4$ were shifted towards higher frequencies. This is indicative of a local preferential conformation. In addition, the Hα and amide protons of $H^6$ were shifted towards higher frequencies.

## Secondary Structural Features of $\alpha_{S2}$-CN(2–20)

The nOes observed for $\alpha_{s2}$-CN(2–20) at a mixing time of 300 ms are summarized in Figure 6. The main structured region comprises the residues of the motif -ΣΣΣEE- based on the secondary Hα chemical shifts and the $d_{NN}(i,i+2)$ crosspeak between $\Sigma^8$ and $\Sigma^{10}$ and $d_{\alpha N}(i,i+4)$ between $\Sigma^9$ and $S^{13}$, and between $\Sigma^{10}$ and $I^{14}$, and $d_{\alpha\beta}(i,i+3)$ between $H^6$ and $\Sigma^9$. Regions of helical structure are characterized by strong $d_{NN}$ connectivities and weak $d_{\alpha N}$ connectivities. Furthermore, a pattern of overlapped $d_{\alpha N}(i,i+4)$, $d_{\alpha\beta}(i,i+3)$, $d_{\alpha N}(i,i+3)$, and either $d_{NN}(i,i+2)$ or $d_{\alpha N}(i,i+2)$ connectivities and evidence of hydrogen bond formation by the amide protons would be expected. Although overlapping connectivities are not present, the $d_{\alpha N}(i,i+4)$, $d_{NN}(i,i+2)$ and $d_{\alpha\beta}(i,i+3)$ nOes suggest nascent α-helix in this region. Earlier CD, ORD and NMR studies of the casein phosphopeptides suggested a lack of α-helical structure [29–31]. Hence this is the first evidence for a tendency to form helical structure in these peptides.

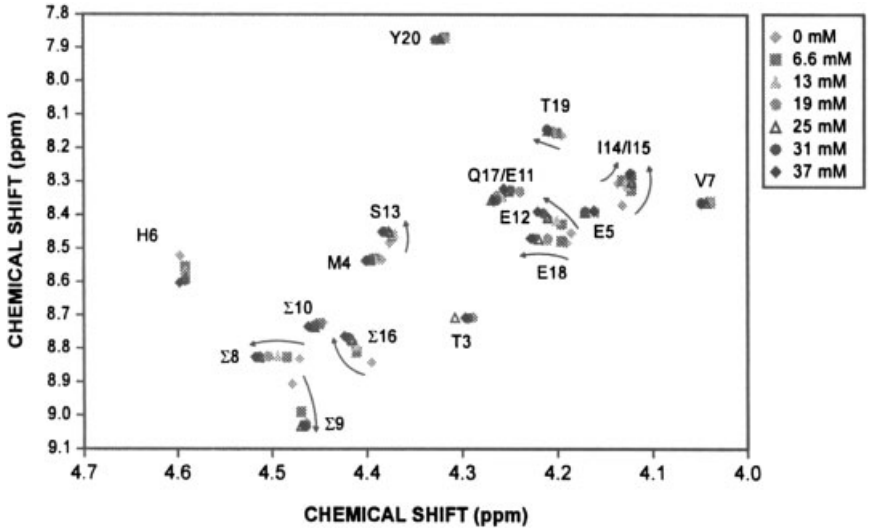


Figure 4 The calcium dependent chemical shift changes in the DQF-COSY fingerprint region of 10.7 mM $\alpha_{S2}$-CN(2–20) at pH 6.36. The residues $H^6$, $\Sigma^8$, $\Sigma^9$, $E^{12}$, $I^{15}$, $\Sigma^{16}$ and $E^{18}$ show significant chemical shift changes in the presence of calcium ions.

Table 1 Chemical Shifts of $\alpha_{S2}$-CN(2–20) at 25 °C and pH 6.30

| Residue | NH | $\alpha$H | $\beta$H | $\gamma$H | Others |
|---|---|---|---|---|---|
| N2 | | 4.36 | 2.86, 2.96 | | 7.03, 7.74 ($\delta NH_2$) |
| T3 | 8.72 | 4.31 | 4.18 | 1.17 | |
| M4 | 8.54 | 4.41 | 1.95, 2.03 | 2.47, 2.54 | 2.02 ($\varepsilon CH_3$) |
| E5 | 8.39 | 4.19 | 1.84, 1.91 | 2.17, 2.19 | |
| H6 | 8.60 | 4.61 | 3.13, 3.13 | | 8.52 (2H), 7.17 (4H) |
| V7 | 8.36 | 4.06 | 1.92 | 0.83, 0.83 | |
| Σ8 | 8.83 | 4.53 | 3.98, 4.14 | | |
| Σ9 | 9.04 | 4.48 | 4.08, 4.08 | | |
| Σ10 | 8.74 | 4.49 | 4.07, 4.07 | | |
| E11 | 8.33 | 4.27 | 1.91, 2.01 | 2.26, 2.26 | |
| E12 | 8.39 | 4.19 | 1.84, 1.91 | 2.17, 2.19 | |
| S13 | 8.45 | 4.40 | 3.78, 3.78 | | |
| I14 | 8.28 | 4.14 | 1.80 | 1.13, 1.40 | 0.85 ($\gamma CH_3$), 0.780 ($\delta CH_3$) |
| I15 | 8.28 | 4.14 | 1.80 | 1.13, 1.40 | 0.85 ($\gamma CH_3$), 0.780 ($\delta CH_3$) |
| Σ16 | 8.78 | 4.44 | 4.01, 4.01 | | |
| Q17 | 8.36 | 4.28 | 1.89, 2.10 | 2.29, 2.29 | 6.86, 7.69 ($\delta NH_2$) |
| E18 | 8.47 | 4.24 | 1.85, 1.90 | 2.15, 2.21 | |
| T19 | 8.14 | 4.23 | 4.08 | 1.074 | |
| Y20 | 7.87 | 4.34 | 2.79, 3.03 | | 7.03 (2,6H), 6.73 (3,5H) |

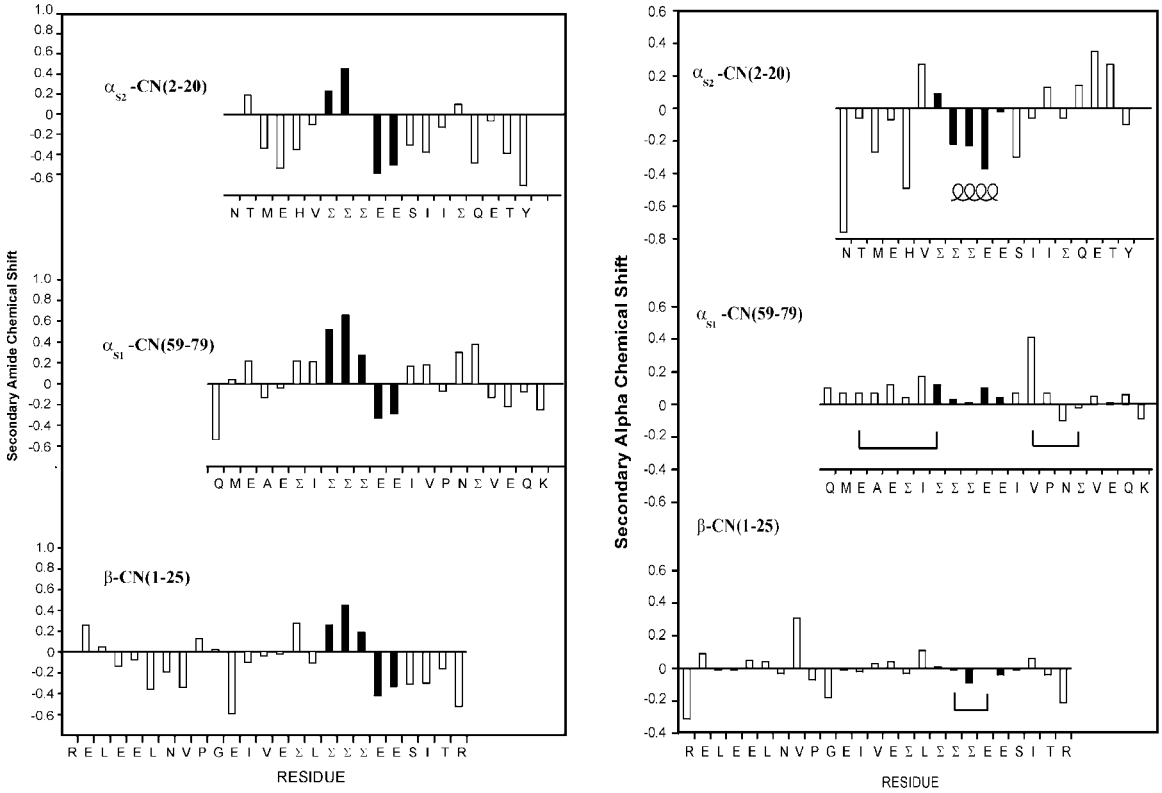


Figure 5 (a) Secondary NH chemical shifts in the presence of molar excess calcium ions of $\alpha_{S2}$-CN(2–20), $\alpha_{S1}$-CN(59–79) [12] and $\beta$-CN(1–25) [11]. (b) Secondary H$\alpha$ chemical shifts in the presence of molar excess calcium ions of $\alpha_{S2}$-CN(2–20), $\alpha_{S1}$-CN(59–79) [12] and $\beta$-CN(1–25) [11] The secondary H$\alpha$ and NH proton chemical shifts of the phosphoseryl residues were calculated using the reported 'random coil' chemical shifts [26,27] and the sequence-dependent corrections [28].

 

The shifted amide protons of $T^3$ and $M^4$ also indicate preferences for local conformations. The nOes from the sidechain of $H^6$ ($H^6$ $^4H$) to $V^7\alpha$, $\Sigma^8\alpha$, $\Sigma^8\beta\beta'$ and $\Sigma^8$NH suggest ion pair formation between the $H^6$ imidazole ring and the nearby phosphate group of $\Sigma^8$. Molecular modelling of the $\alpha_{S2}$-CN(2–20) peptide, based on the nOes shown in Figure 6, shows that the constraints are not sufficient to confine it to a unique conformation. However, analysis of the individual conformers suggest nascent helix within the region $^9\Sigma\Sigma EE^{12}$. The heavy backbone atoms of residues $^9\Sigma\Sigma EE^{12}$ of the ten lowest energy conformers superimposed with an RMSD of 0.9 Å is illustrated in Figure 7.

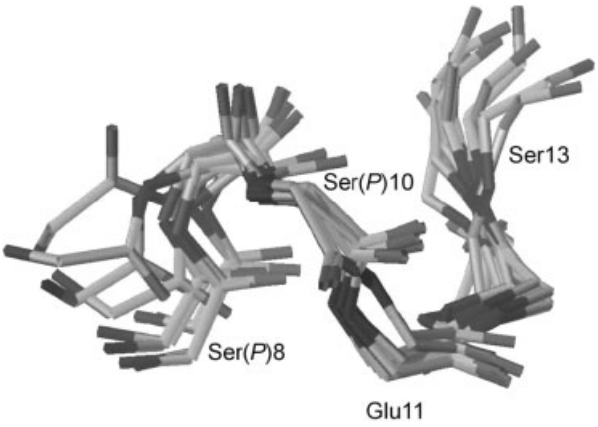


Figure 7 Superimposition of ten lowest energy structures determined based on simulated annealing using the nOe constraints in Figure 5, illustrating the propensity of these residues to adopt a helical conformation.

## Comparison of Secondary Structural Features of $\alpha_{S2}$-CN(2–20), $\alpha_{S1}$-CN(59–79) and $\beta$-CN(1–25)

The secondary H$\alpha$ and NH proton chemical shifts of the three peptides $\alpha_{S1}$-CN(59–79) [12], $\beta$-CN(1–25) [11] and $\alpha_{S2}$-CN(2–20) are shown in Figure 5(a,b) highlighting the $\Sigma\Sigma\Sigma EE$ motif. Figure 6 shows the comparison of the non-sequential nOes for the three multi-phosphorylated peptides with the -$\Sigma\Sigma\Sigma EE$- region aligned. Within the -$\Sigma\Sigma\Sigma EE$- region, the

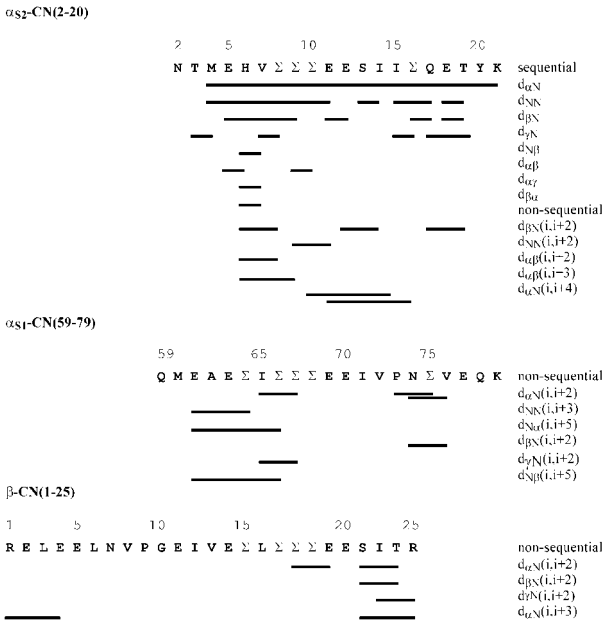


Figure 6 Summary of spectral data for $\alpha_{S2}$-CN(2–20) and comparison with the non-sequential nOes for $\alpha_{S1}$-CN(59–79) and $\beta$-CN(1–25). The sequential, medium-range and long-range nOes are depicted using bars. The asterisks indicate nOes that were not observed due to spectral congestion. The three sequences are aligned for maximum homology in the $\Sigma\Sigma\Sigma EE$ region.

$d_{NN}(i,i+1)$ nOe between $\Sigma^9$ and $E^{11}$ of $\alpha_{S2}$-CN(2–20) was observed at 400 MHz. In contrast, in $\beta$-CN(1–25), a medium range nOe was observed between the H$\alpha$ proton of $\Sigma^{16}$ and amide proton of $E^{20}$ [11]. Our evidence for turns and loops in the two peptides $\alpha_{S1}$-CN(59–79) and $\beta$-CN(1–25) is consistent with the report by Small *et al.* [32] who examined 14 different highly phosphorylated proteins, and found that 80% of the phosphorylated sites existed within regions predicted to be $\beta$-turns.

In summary, the spectral data of the three multiphosphorylated casein peptides indicates that all three peptides have specific, folded conformations in the presence of calcium. However, despite the sequence homology, there is variability in the local conformations in the -$\Sigma\Sigma\Sigma EE$- region and the conformation is strongly influenced by the neighbouring residues.

## Acknowledgement

We wish to thank David Stanton for purification of the peptides. This work was supported by an NH&MRC project grant 209042 and the Dairy Research and Development Corporation of Australia.

## REFERENCES

1. Roach PJ. Multisite and hierarchal protein phosphorylation. *J. Biol. Chem* 1991; **266**: 14 139–14 142.

2. ANGIS. The Australian National Genomic Information Service, 1994.
3. Reeves RE. Calcium phosphate sequestering phosphopeptide from casein. *Science* 1958; **128**: 472.
4. Lee YS, Noguchi T, Naito H. Phosphopeptides and soluble calcium in the small intestine of rats given a casein diet. *Br. J. Nutr* 1980; **43**: 457–467.
5. Sato R, Noguchi T, Naito H. Casein phosphopeptide (CPP) enhances calcium absorption from the ligated segment of rat small intestine. *J. Nutr. Sci. Vitaminol* 1986; **32**: 67–76.
6. Kasai T, Iwasaki R, Tanaka M, Kiriyama S. Casein-phosphopeptides (CPP) in feces and contents in digestive tract of rats fed casein and CPP preparations. *Biosci. Biotech. Biochem* 1995; **59**: 26–30.
7. Ferraretto A, Signorile A, Gravaghi C, Fiorilli A, Tettamanti G. Casein phosphopeptides influence calcium uptake by cultured human intestinal HT-29 tumor cells. *J. Nutr* 2001; **131**: 1655–1661.
8. Reynolds EC. Remineralization of enamel subsurface lesions by casein phosphopeptide-stabilized calcium phosphate solutions. *J. Dent. Res* 1997; **76**: 1587–1595.
9. Reynolds EC, Black CL, Cai F, Cross KJ, Eakins D, Huq NL, Morgan MV, Nowicki A, Perich JW, Riley PF, Shen P, Talbo G, Webber F. Advances in enamel remineralization: Casein phosphopeptide-amorphous calcium phosphate. *J. Clin. Dent* 1999; **10**: 86–88.
10. Reynolds EC, Cain CJ, Webber FL, Johnson IH, Perich JW. Anticariogenicity of calcium phosphate complexes of tryptic casein phosphopeptides in the rat. *J. Dent. Res* 1995; **74**: 1272–1279.
11. Cross KJ, Huq NL, Bicknell W, Reynolds EC. Cation-dependent structural features of beta-casein-(1–25). *Biochem. J* 2001; **356**: 277–285.
12. Huq NL, Cross KJ, Reynolds EC. A $^{1}$H-NMR study of the casein phosphopeptide alpha s1-casein(59–79). *Biochim. Biophys. Acta* 1995; **1247**: 201–208.
13. Reynolds EC, Riley PF, Adamson NJ. A selective precipitation procedure for the purification of multiple-phosphoseryl containing peptides and their identification. *Anal. Biochem* 1994; **217**: 277–284.
14. Adamson N, Riley PF, Reynolds EC. The analysis of multiple phosphoseryl-containing casein peptides using capillary zone electrophoresis. *J. Chromatogr. A* 1993; **646**: 391–396.
15. Talbo GH, Suckau D, Malkoski M, Reynolds EC. MALDI-PSD-MS analysis of the phosphorylation sites of caseinomacropeptide. *Peptides* 2001; **22**: 1093–1098.
16. Marion D, Ikura M, Tschudin R, Bax A. Rapid recording of 2D NMR spectra without phase cycling. Application to the study of hydrogen exchange in proteins. *J. Magn. Reson* 1989; **85**: 393–399.
17. Smallcombe SH, Patt SL, Keifer PA. WET solvent suppression and its applications to LC NMR and high-resolution NMR spectroscopy. *J. Magn. Reson., Ser. A* 1995; **117**: 295–303.
18. Jeener J, Meier BHA, Bachmann P, Ernst RR. Investigation of exchange processes by two-dimensional NMR spectroscopy. *J. Chem. Phys* 1979; **71**: 4546–4553.
19. Macura S, Huang Y, Suter D, Ernst RR. Two-dimensional chemical exchange and cross-relaxation spectroscopy of coupled nuclear spins. *J. Magn. Reson* 1981; **43**: 259–281.
20. Bax A, Davis DG. MLEV-17-based two-dimensional homonuclear magnetization transfer spectroscopy. *J. Magn. Reson* 1985; **65**: 355–360.
21. Braunschweiler L, Ernst RR. Coherence transfer by isotropic mixing: Application to proton correlation spectroscopy. *J. Magn. Reson* 1983; **53**: 521–528.
22. Piantini U, Sørensen OW, Ernst RR. Multiple quantum filters for elucidating NMR coupling networks. *J. Am. Chem. Soc* 1982; **104**: 6800–6801.
23. Shaka AJ, Freeman R. Simplification of NMR spectra by filtration through multiple-quantum coherence. *J. Magn. Reson* 1983; **51**: 169–173.
24. Ernst RR, Bodenhausen G, Wokaun A. *Principles of Nuclear Magnetic Resonance in One and Two Dimensions*. Clarendon Press: Oxford, 1990.
25. Wüthrich K. *NMR of Proteins and Nucleic Acids*. Wiley and Sons: New York, 1986.
26. Bienkiewicz EA, Lumb KJ. Random-coil chemical shifts of phosphorylated amino acids. *J. Biomol. NMR* 1999; **15**: 203–206.
27. Merutka G, Dyson HJ, Wright PE. 'Random coil' $^{1}$H chemical shifts obtained as a function of temperature and trifluoroethanol concentration for the peptide series GGXGG. *J. Biomol. NMR* 1995; **5**: 14–24.
28. Schwarzinger S, Kroon GJ, Foss TR, Chung J, Wright PE, Dyson HJ. Sequence-dependent correction of random coil NMR chemical shifts. *J. Am. Chem. Soc* 2001; **123**: 2970–2978.
29. Holt C, Sawyer L. Primary and predicted secondary structures of the caseins in relation to their biological functions. *Protein Eng* 1988; **2**: 251–259.
30. Humphrey RS, Jolley KW. 31P-NMR studies of bovine beta-casein. *Biochim. Biophys. Acta* 1982; **708**: 294–299.
31. Sleigh RW, Mackinlay AG, Pope JM. NMR studies of the phosphoserine regions of bovine alpha s1- and beta- casein. Assignment of$^{31}$P resonances to specific phosphoserines and cation binding studied by measurement of enhancement of $^{1}$H relaxation rate. *Biochim. Biophys. Acta* 1983; **742**: 175–183.
32. Small D, Chou PY, Fasman GD. Occurrence of phosphorylated residues in predicted $\beta$-turns. Implications for $\beta$-turns participation in control mechanisms. *Biochem. Biophys. Res. Commun* 1977; **79**: 341–346.

 